Electronic Supporting Information

Characterization of 2'-deoxyguanosine oxidation products observed in the Fenton-like system Cu(II)/H_2O_2/reductant in nucleoside and oligodeoxynucleotide contexts

Aaron M. Fleming, James G. Muller, Insun Ji, Cynthia J. Burrows*

Department of Chemistry, University of Utah, Salt Lake City, UT 84112-0850

Email: burrows@chem.utah.edu

Table of Contents

General Section-

HPLC Analysis:

Analysis of the reactions was conducted by passing the sample down a C18 reversed-phase HPLC column (250 X 4.6 mm, 5 μm) running the following solvents: A = 10 mM NH_4OAc (pH 7.0) in ddH_2O, B = CH_3CN, running at 1 mL/min, while monitoring the absorbance at 240 nm. The run was initiated at 1% B then after 3 min B increased to 10% over 10 min following a linear gradient, after which 10% B was held isocratic for 4 min. Next, B was increased to 65% over 10 min along a linear gradient then held at 65% for 10 min followed by termination of the run. The void volume from this HPLC run was collected and lyophilized to dryness. The LC-MS analysis was conducted with a smaller C18 HPLC column (250 X 2.1 mm, 3 μm) running A = 2 mM NH_4OAc (pH 7.0) and B = CH_3CN, running the same method above; therefore, the LC-MS and analyzed HPLC trace retention times do not lineup.

Analysis of the void volume from the previous run was achieved by passing the collected sample down a Hypercarb HPLC column (150 X 4.6 mm, 5 μm, Thermo Scientific) that was running the following solvent systems: A = 0.1% acetic acid in ddH_2O, and B = methanol, while running at a 1 mL/min flow rate, and monitoring absorbance at 240 nm. The run started at 0% B and after 10 min increased to 90% B following a linear gradient over 30 min. The LC-MS analysis was conducted with a smaller Hypercarb HPLC column (100 X 2.1 mm, 5 μm, Thermo Scientific); therefore, the retention times do not lineup between the LC-MS studies and the analyzed chromatograms shown below.

Mass spectrometry analysis of deoxynucleoside products:

Free Base fragmentation by ESI^+-MS/MS. The nucleoside samples were analyzed by positive ion electrospray ionization (ESI) on a Micromass Quattro II tandem mass spectrometer equipped with Zspray API source. Samples were dissolved in CH_3CN and 0.1% formic acid ddH_2O (1:1) and introduced via infusion at a flow rate of 7 μL/min. The source and desolvation temperatures were 80 ^oC and 120 ^oC, respectively. The capillary voltage was set to 3.25 KV, sampling cone voltage to 45 V, and the extractor cone to 3 V. The collision energy was set to 18 eV. Argon, used as a gas collision for CID experiments, was adjusted to a pressure of 1.7 X 10-4 mVar. The mass for the nucleoside base was set in the first scanning analyzer (MS-1) and the precursor ion was subjected to CID in the static quadrupole and the resulting spectrum of the products recorded by scanning the second scanning analyzer (MS-2) between 50 and 600 Da. The scan duration and interscan delay were 3.0 and 0.1 seconds, respectively. The instrument was operated and data accumulated with Micromass Masslynx software (version 4.0).

Accurate mass measurements were made by positive electrospray ionization (ESI) on a Waters LCT XE Premier TOF mass spectrometer equipped with a Zspray API source using 0.03% phosphoric acid as the LockSpray analyte. The source and desolvation temperatures were 85 ^oC and 185 ^oC, respectively. The capillary voltage was set to 2.0 kV, sampling cone voltage to 100 V. The instrument was operated and data accumulated with Micromass MassLynx software (version 4.1).

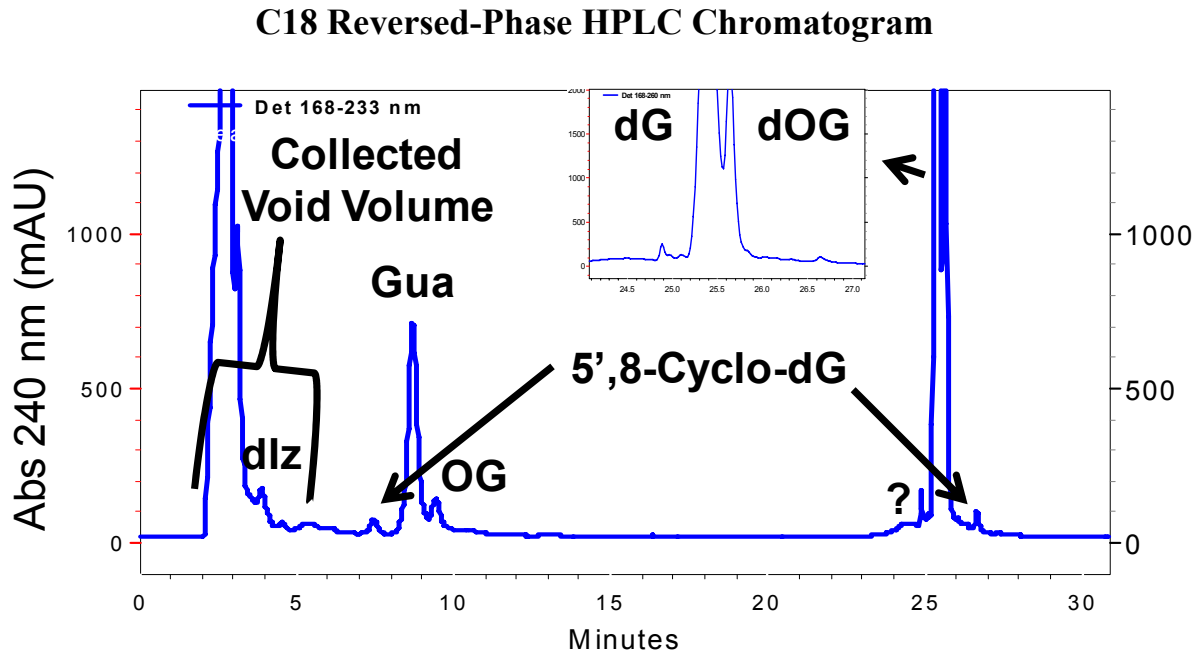

Figure S1. Typical C18 RP-HPLC traces to analyze **dG** oxidation products from Cu-mediated oxidation.

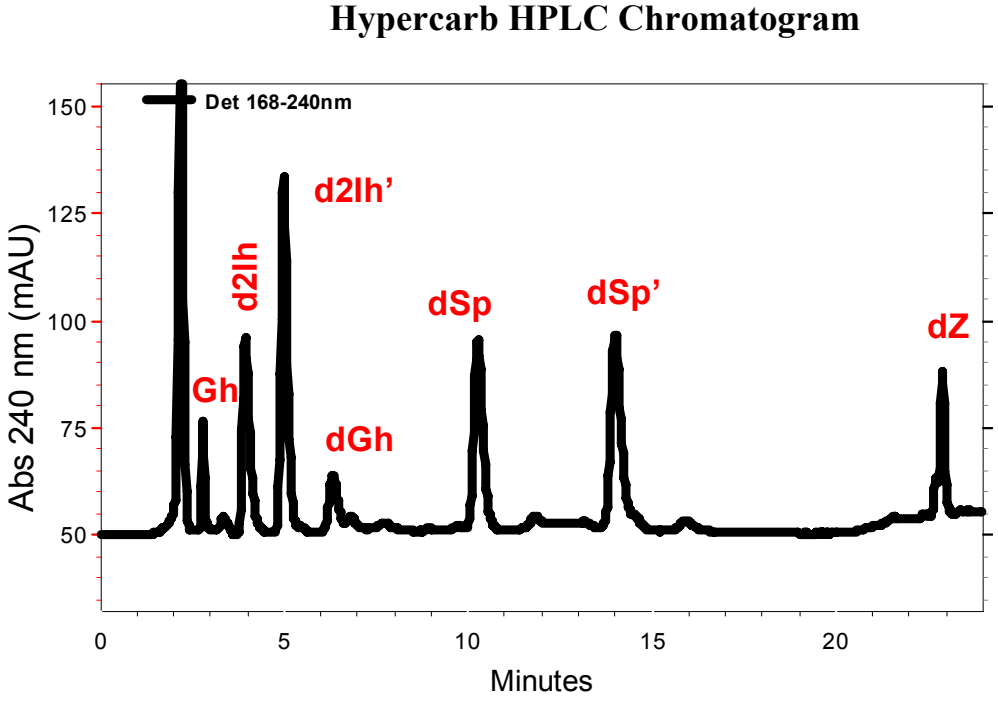

Figure S2. Typical Hypercarb HPLC traces to analyze **dG** oxidation products from Cu-mediated oxidation.

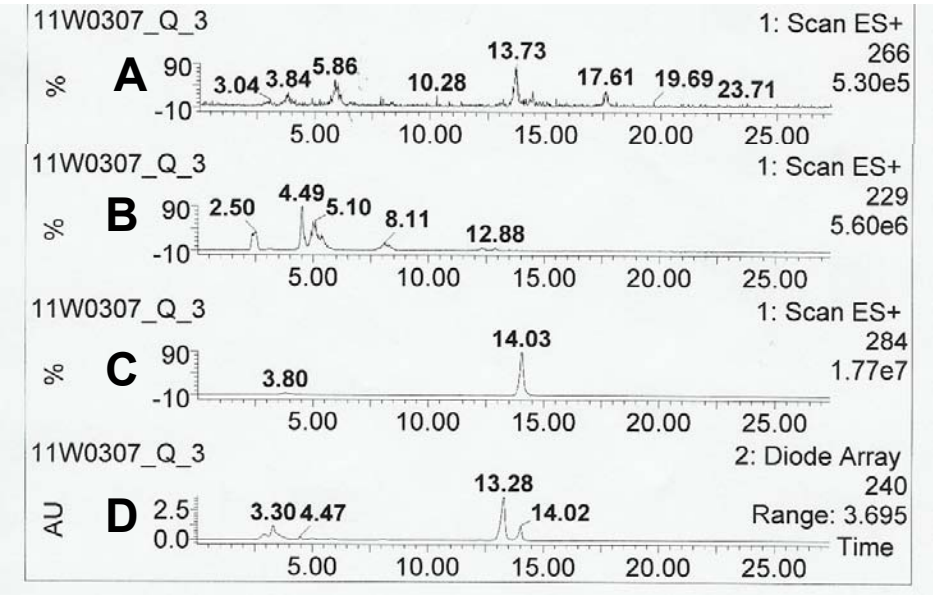

Figure S3. LC-ESI$^+$-MS analysis for nucleoside products observed from **dG** oxidation with Cu(II)/H_2O_2/Asc on the C18 RP-HPLC column. Panel A = **5',8-cyclo-dG**, B = **dIz**, C = **dOG**, and D = Abs at 240 nm.

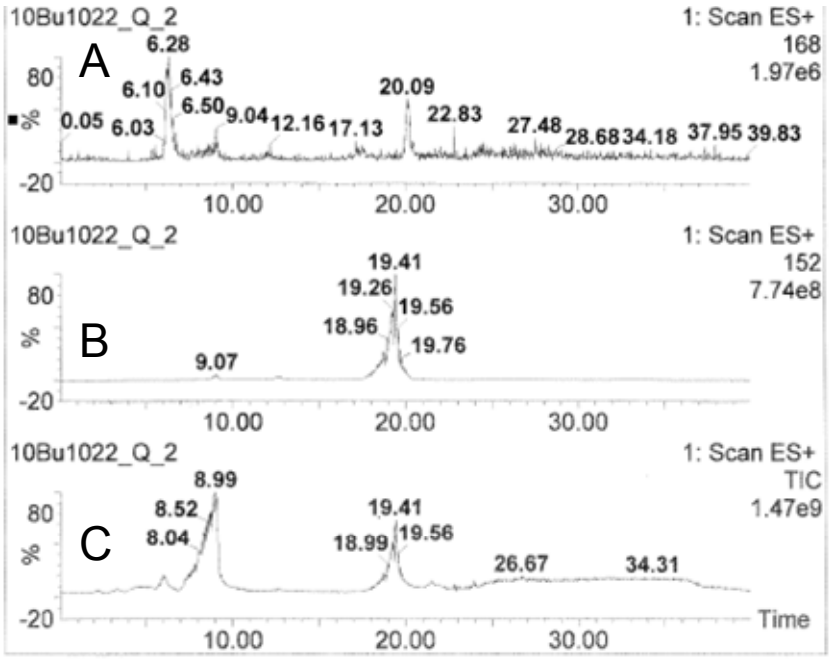

Figure S4. LC-ESI$^+$-MS analysis for free base products observed from **dG** oxidation with Cu(II)/H_2O_2/Asc on the C18 RP-HPLC column. Panels A = **OG**, B = **Gua**, and C = TIC spectra.

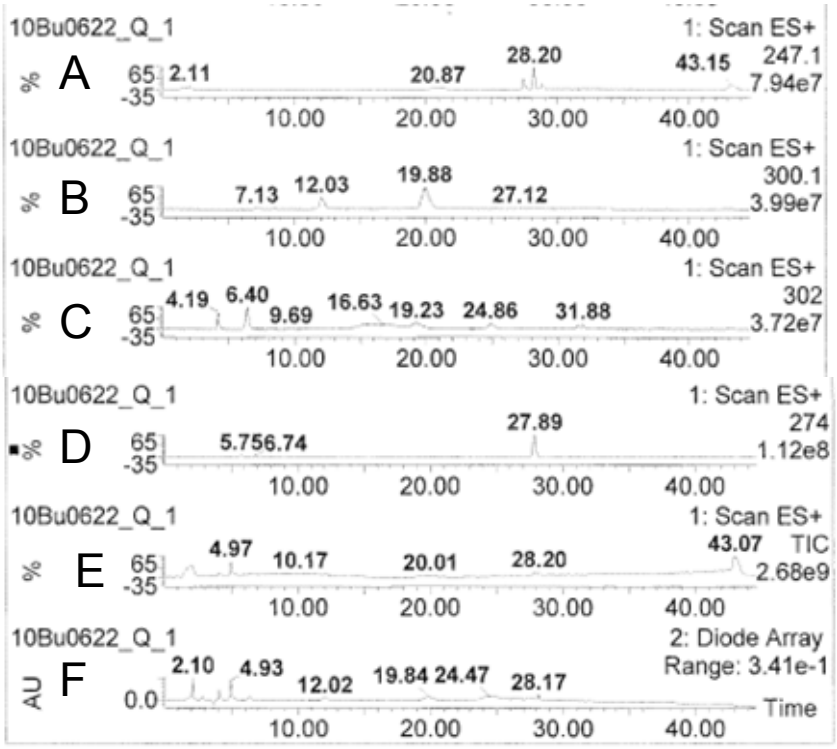

Figure S5. LC-ESI$^+$-MS analysis (Hypercarb column, 100 X 2.1 mm) for nucleoside products observed from **dG** oxidation with Cu(II)/H_2O_2/Asc. Panels A = **dZ**, B = **dSp**, and C = **d2Ih**, D = **dGh**, E = TIC spectra, and F = Abs at 240 nm.

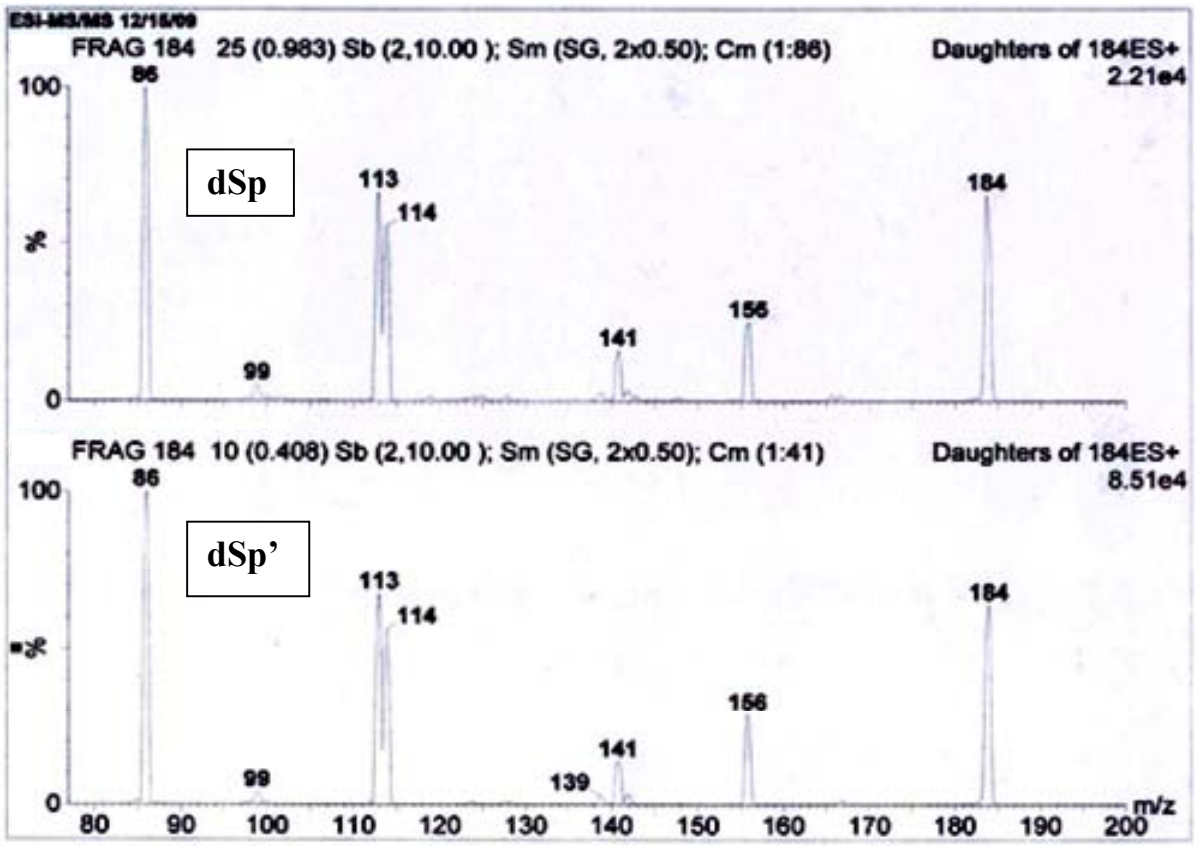

Figure S6. ESI^+-MS/MS free-base fragmentation data for the **dSp** diastereomers, **dSp** and **dSp'** (free-base mass $(M+H)^+ = 184$). Compared to the values published in the following reference. $(M+H)^+ = 184$, 156, 141, 113, 86. Luo, W.; Muller, J.G.; Burrows, C.J. *Org. Letts.* **2000**, *2*, 613-616.

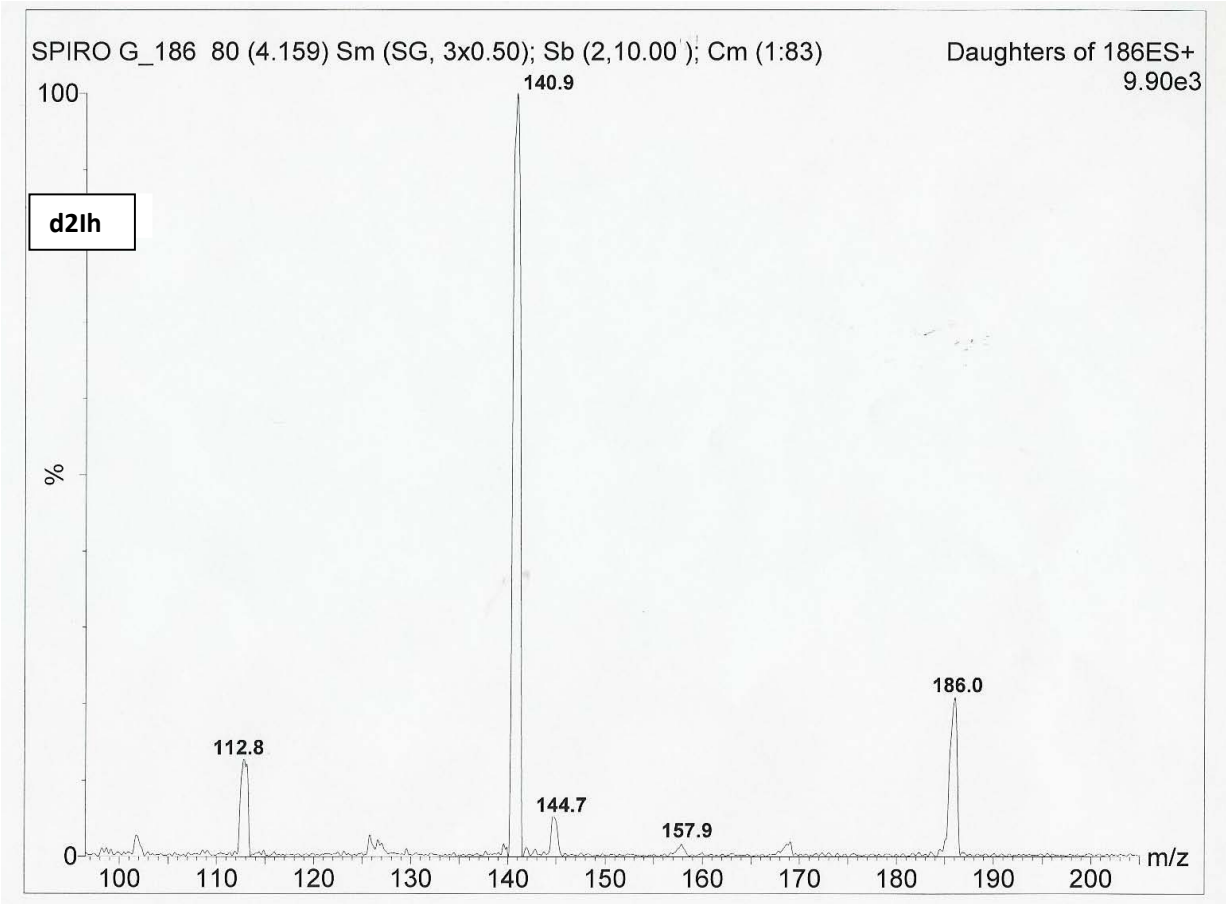

Figure S7. ESI^+-MS/MS free-base fragmentation data for a mixture of the **d2Ih** diastereomers (free-base mass $(M+H)^+ = 186$). Compared to the values found in the following reference. $(M+H)^+ = 186, 158, 141$. Ye, W.; et. al. *J. Am. Chem. Soc*. **2009**, *131*, 6114-6123.

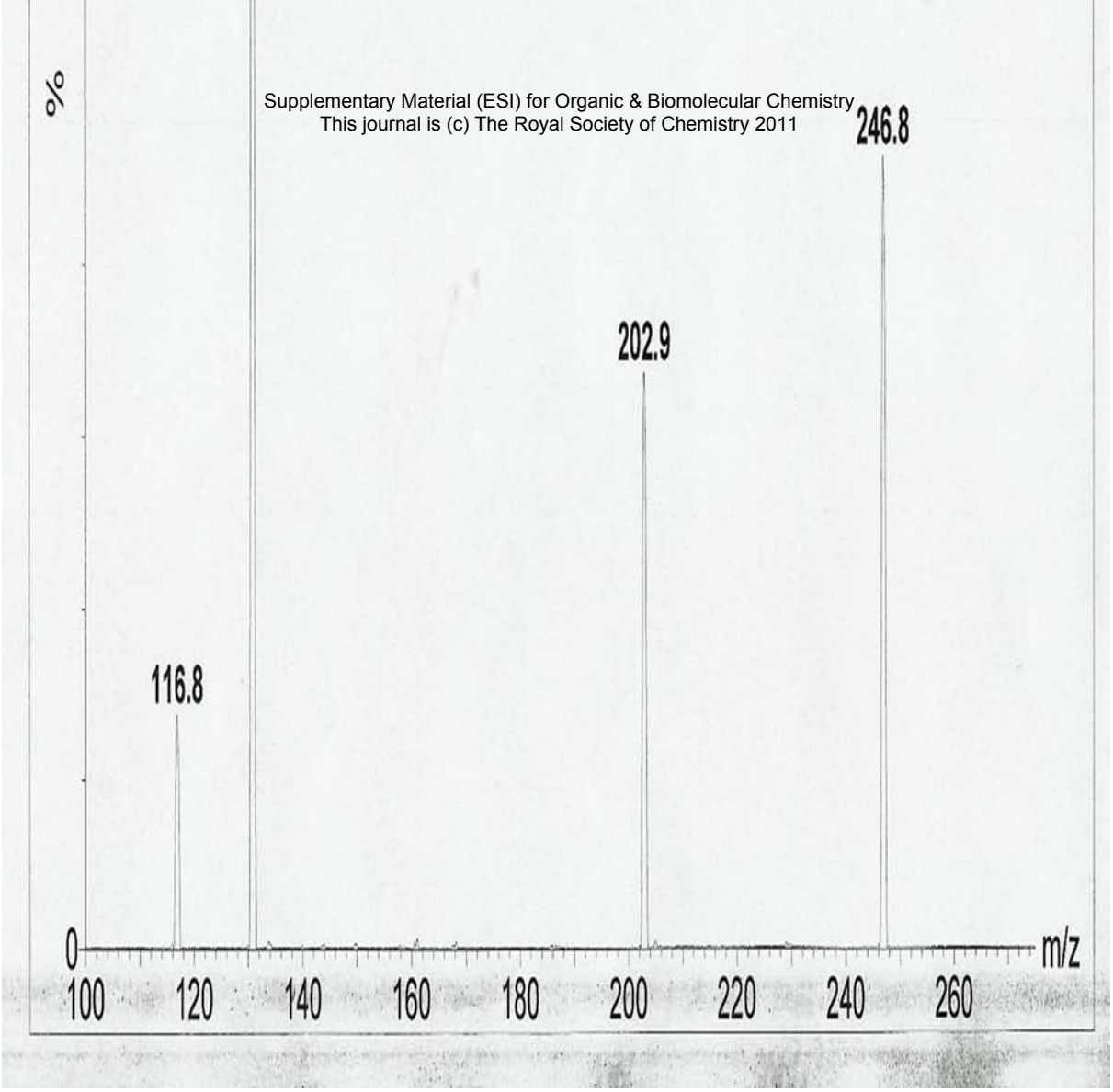

Figure S8. ESI^+-MS/MS for **dZ** nucleoside. The data was compared to the values found in the following reference. $(M+H)^+$ = 247, 203, and 131. Matter, B.; Malejka-Giganti, D.; Csallany, A.S.; Tretyakova, N. *Nucleic Acids Res.* **2006**, *34*, 5449-5460.

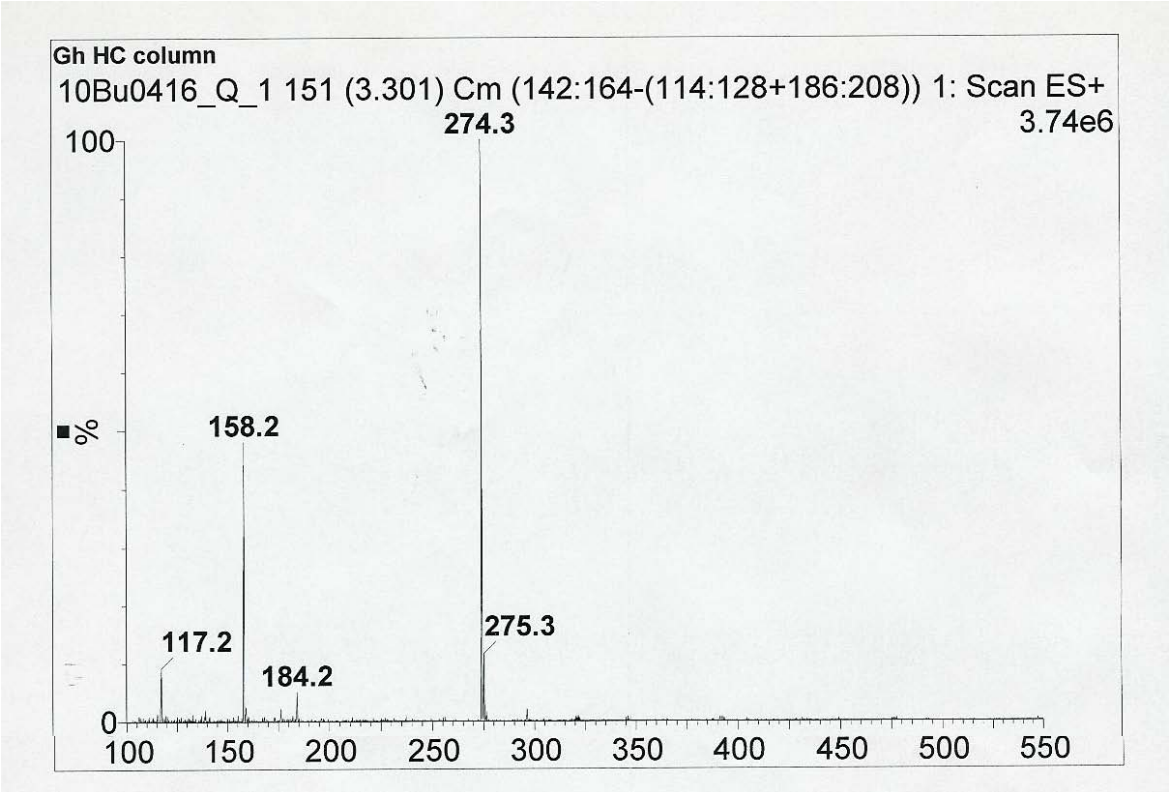

Figure S9. ESI^+-MS for **dGh**. The calculated $(M+H)^+ = 274.3$.

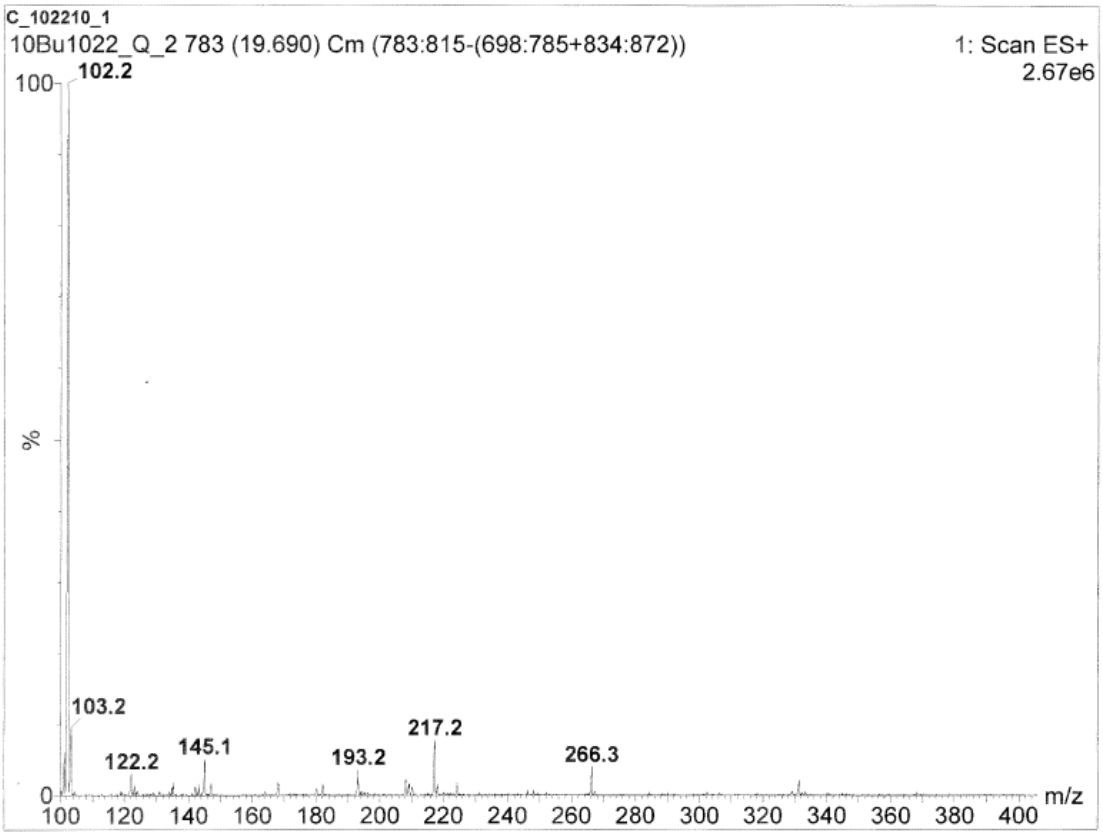

Figure S10. ESI^+-MS for **5',8-Cyclo-dG**. The calculated value $(M+H)^+ = 266.2$.

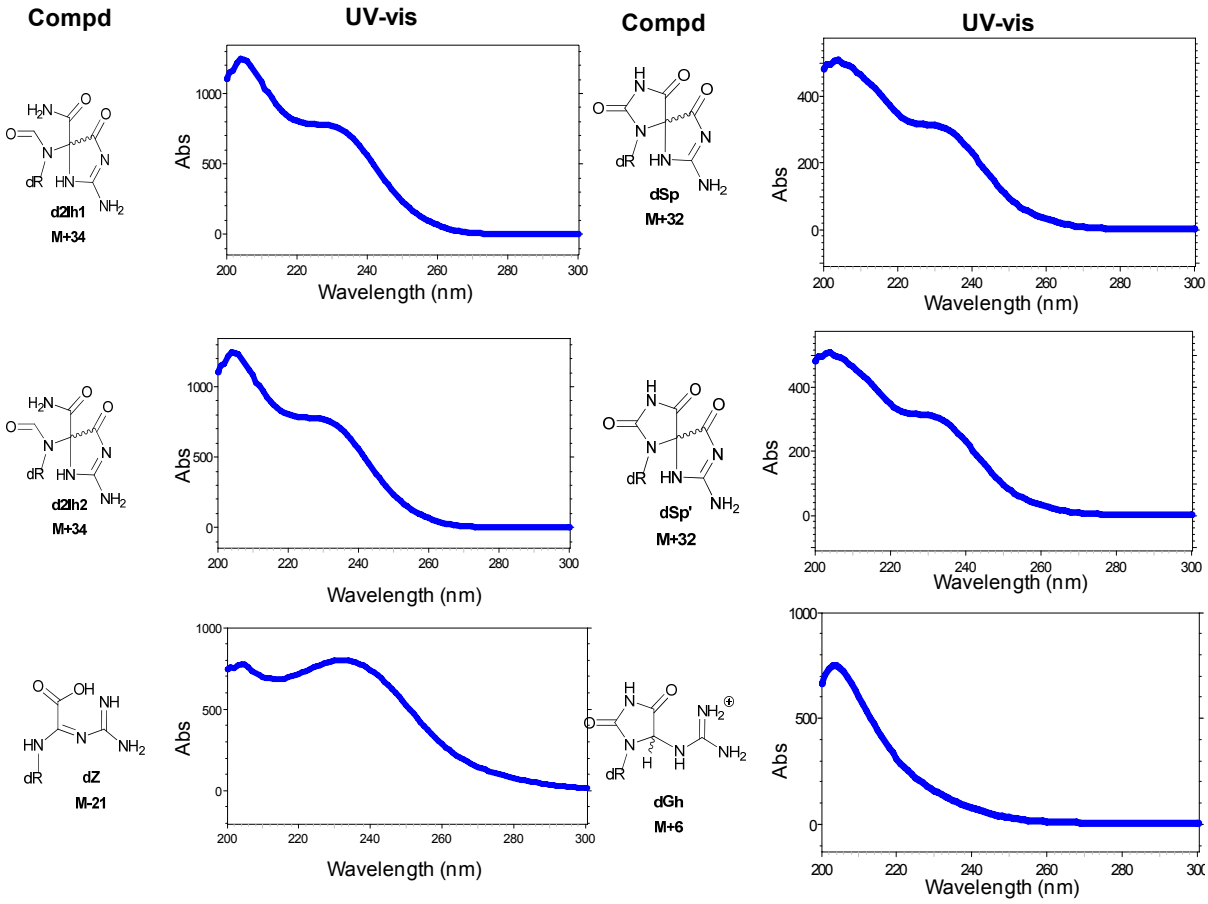

Figure S11. UV-vis spectra for the two diastereomers of **d2Ih**, two diastereomers of **dSp**, **dGh**, and **dZ**.

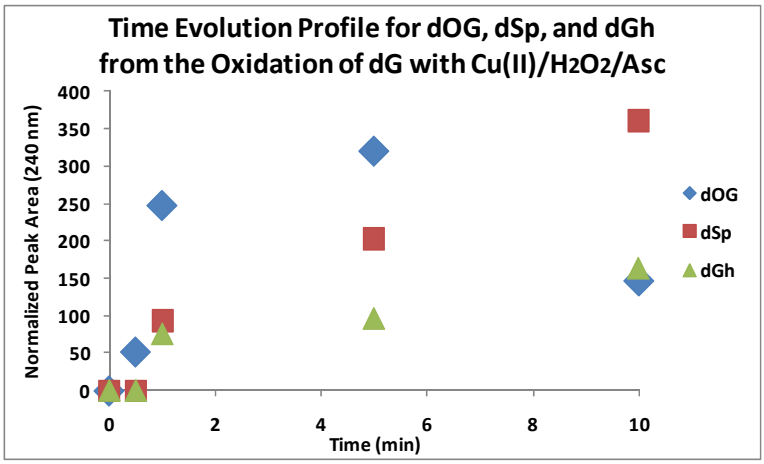

C8-Oxidation Products

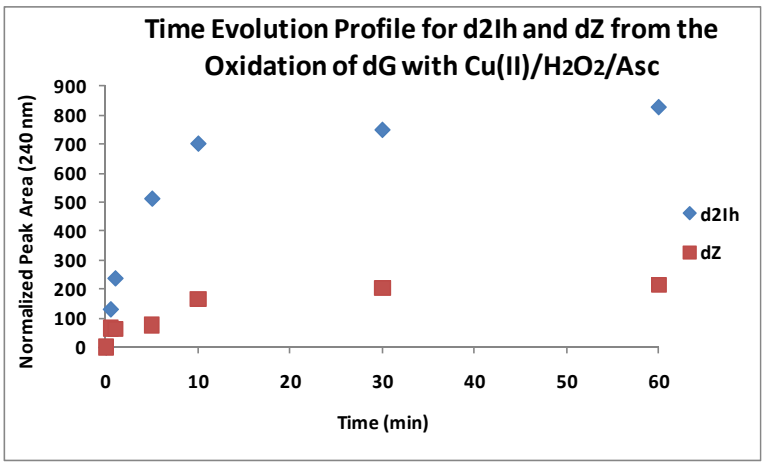

C5-Oxidation Products

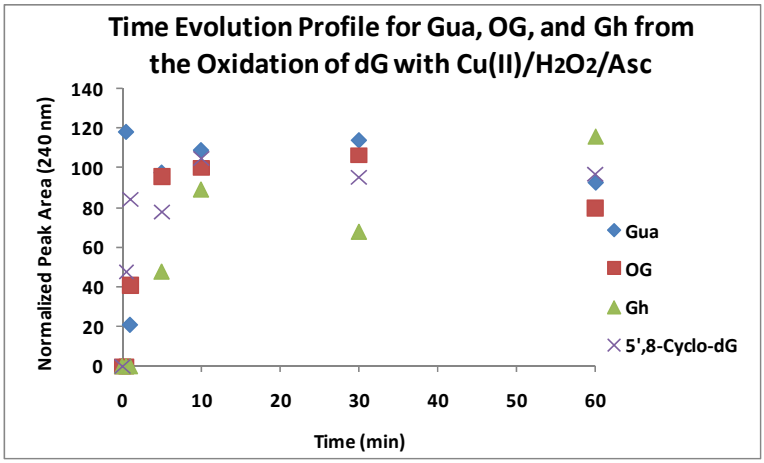

Sugar-Oxidation Products

Figure S12. Time evolution profiles for products observed from the oxidation of **dG** with Cu(II)/H_2O_2/Asc. The time profile for **dOG**, **dSp**, and **dGh** is only shown out to 10 min to emphasize the how the products change with time in the beginning of the reaction. The profiles for C5 products and base-oxidation products are shown out to 60 min.

	Absolute Product Yield-Cu(II)/H_2O_2/Asc						
	Relative Yields			Relative Yield		Absolute Yield[a]	
	Trl 1	Trl 2	Trl 3	Ave	Std Dev	Ave	Std Dev
Gua	23.42712	21.30305	25.61816	23.44945	2.15764	8.51215	0.78322
OG	7.09477	7.29157	7.49594	7.29409	0.20060	2.64776	0.07282
Gh	0.87374	0.89798	0.40129	0.72434	0.28003	0.26294	0.10165
dOG	14.83930	15.25093	14.45548	14.84857	0.39780	5.39003	0.14440
dZ	3.00996	3.09346	2.70646	2.93663	0.20366	1.06600	0.07393
d2Ih	32.74689	33.65526	31.67388	32.69201	0.99183	11.86720	0.36003
dSp	12.99083	13.35119	12.80878	13.05027	0.27605	4.73725	0.10020
dGh	2.06251	2.11972	2.00523	2.06249	0.05725	0.74868	0.02078
5',8-Cyclo-dG	2.95487	3.03683	2.83476	2.94216	0.10163	1.06800	0.03689
dGh_{red}	0.00000	0.00000	0.00000	0.00000	0.00000	0.00000	0.00000

	Absolute Product Yield-Cu(II)/H_2O_2/NAC						
	Relative Yields			Relative Yield		Absolute Yield[b]	
	Trl 1	Trl 2	Trl 3	Ave	Std Dev	Ave	Std Dev
Gua	18.24744	22.26426	19.43349	19.98173	2.06377	6.25428	0.64596
OG	0.00000	0.00000	0.00000	0.00000	0.00000	0.00000	0.00000
Gh	0.00000	0.00000	0.00000	0.00000	0.00000	0.00000	0.00000
dOG	8.67595	8.27874	8.25814	8.40428	0.23550	2.63054	0.07371
dZ	1.55753	1.30045	1.41593	1.42464	0.12876	0.44591	0.04030
d2Ih	58.38127	56.03698	57.88334	57.43386	1.23509	17.97680	0.38658
dSp	9.34943	8.92555	9.17672	9.15057	0.21315	2.86413	0.06672
dGh	2.67613	2.04753	2.74040	2.48802	0.38283	0.77875	0.11982
5',8-Cyclo-dG	1.11225	1.14648	1.09198	1.11690	0.02755	0.34959	0.00862
dGh_{red}	0.00000	0.00000	0.00000	0.00000	0.00000	0.00000	0.00000

[a] Based on an average overall yield of 36.3%.

[b] Based on an average overall yield of 31.3%.

Figure S13. These tables show the data collected from the three nucleoside trials. The table on the top provides data collected with the reductant Asc, and the bottom table shows data collected with the reductant NAC. The data is shown with relative and absolute yields along with the standard deviation, which was used for the error bars.

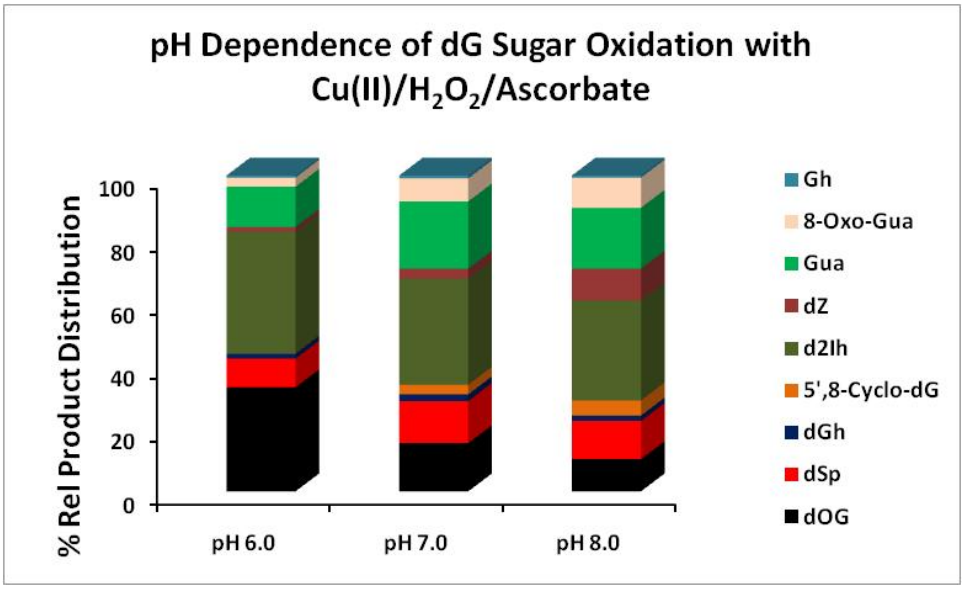

Figure S14. pH dependence in the observed product distribution from oxidation of **dG** nucleoside with Cu(II)/H_2O_2/Asc at pH 6.0, 7.0, and 8.0.

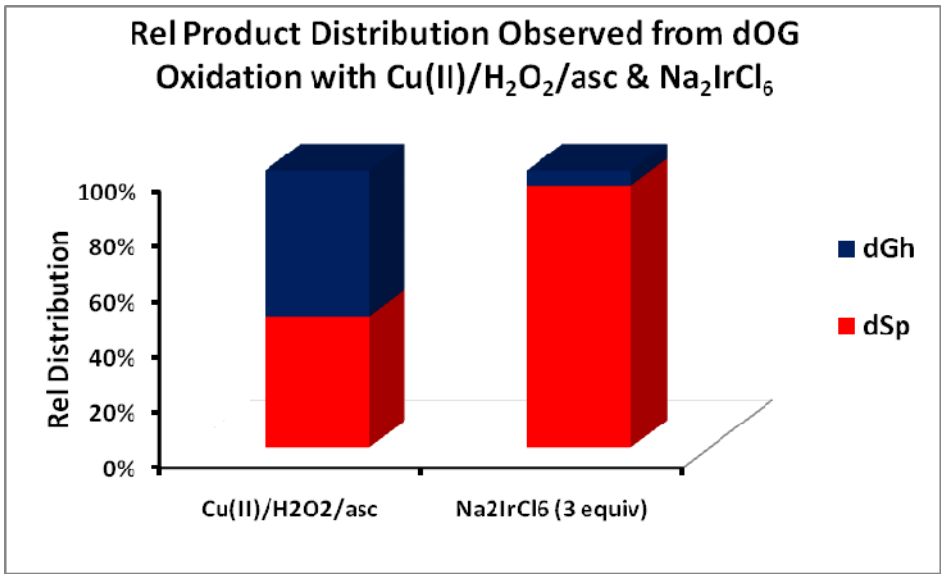

Figure S15. This chart provides the product distribution observed when **dOG** (2.0 mM) allowed to react with Cu(II)/H_2O_2/Asc (1.0 mM, 10 mM, and 2.0 mM) in NaP_i buffer (75.0 mM, pH 7.0) for 1 h at 22 °C. This data was compared to the known reaction between **dOG** (2.0 mM) and Na_2IrCl_6 (6.0 mM) under the same conditions. Luo, W.; Muller, J.G.; Burrows, C.J. *Org. Letts.* **2000**, *2*, 613-616.

dOG oxidation studies with riboflavin, oxyl radicals, and $^1O_2$were shown to also yield dehydroguanidinohydantoin (**dGh^{ox}**) and its decomposition products oxaluric acid (**dOa**) that further decomposes to urea(**dUa**, see Scheme below); under these HPLC separation conditions, dGhox would not be observed (due to its decomposition), but **dOa** and **dUa** can be detected. **dOa** and **dUa** have been observed from other reactions in our laboratory using the outlined chromatography in this study, but these products were not observed in detectable yields in these studies. Because reaction quantification was achieved following product absorbance at 240 nm, and not HPLC-MS, the **dUa** lesion could not be detected, and a peak consistent with **dOa** was not observed. Based on the mass balance errors, the combined yield of **dOa** and **dUa** cannot exceed an absolute yield greater than 1.6-1.8%. Because these products are a result of a 6-electron oxidation, their likely hood of occurring before a repair event occurs is very low. This pathway is reviewed in Neeley, W.L.; Essigmann, J.M. *Chem. Res. Toxicol.* **2006**, *19*, 491-505.

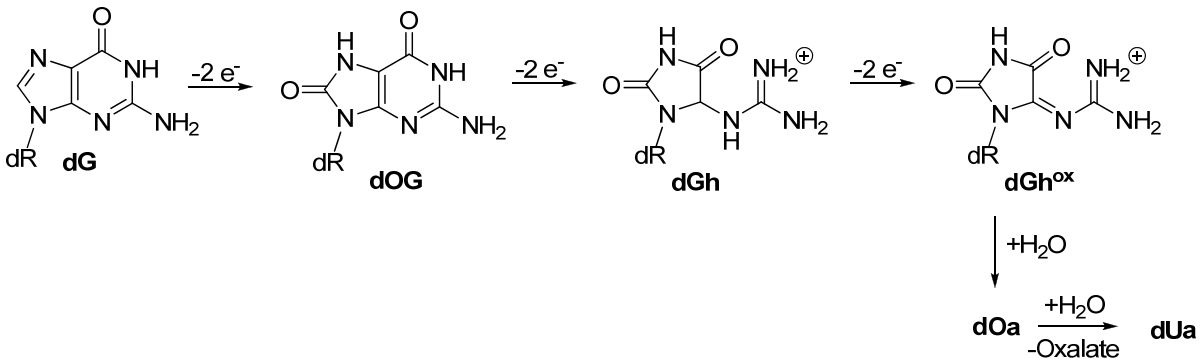

Figure S16. The above scheme and description describe the over-oxidation products that have been observed from dG oxidation in previous studies, but were not detected in the oxidations outlined in this text.

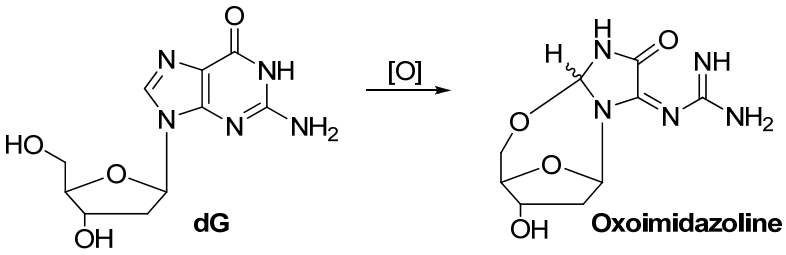

We have observed oxoimidazoline (MW 255) from **dG** oxidation with riboflavin following a similar reaction setup as utilized by the Cadet laboratory (*JACS*, **2003**, *125*, 2030). When **dG** was oxidized with Cu-mediated oxidants a peak and mass were not observed for oxoimidazoline. The mechanisms outlined in Schemes 3 and 4B that show **dG** base oxidation occurring by an N7 coordinated Cu complex suggest direct addition of an OH group to either C5 or C8. This coordination complex would remain until protonation of the N7 nitrogen occurs, releasing the Cu. This coordinated complex could prevent the 5'-OH from attacking C8 leading to oxoimidazoline.

Figure S17. Oxoimidazoline formation and a possible explanation for not observing it in these studies.

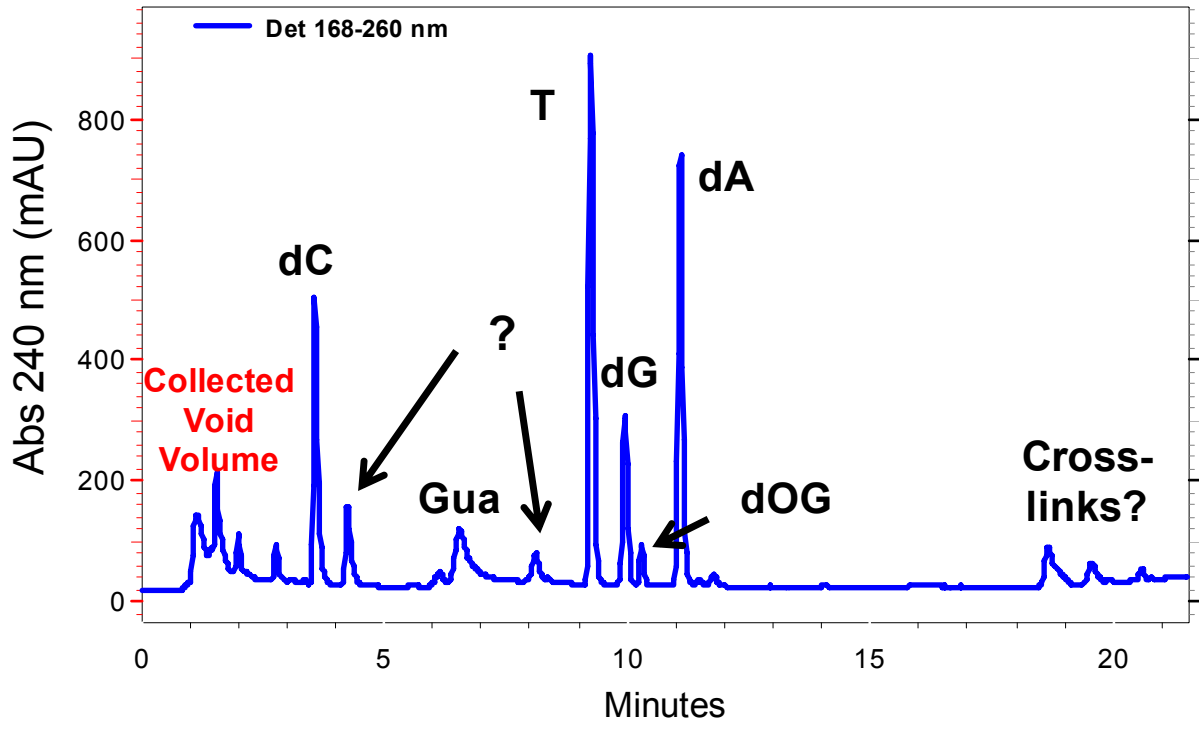

Figure S18. C18 Reversed-Phase HPLC Chromatogram for the Digested **ODN-12** Oxidation Reaction. The peaks labeled with a question mark at 4 and 8 min have the same retention times and UV-vis characteristics as the Thy (4 min) and Ade (8 min) free bases.

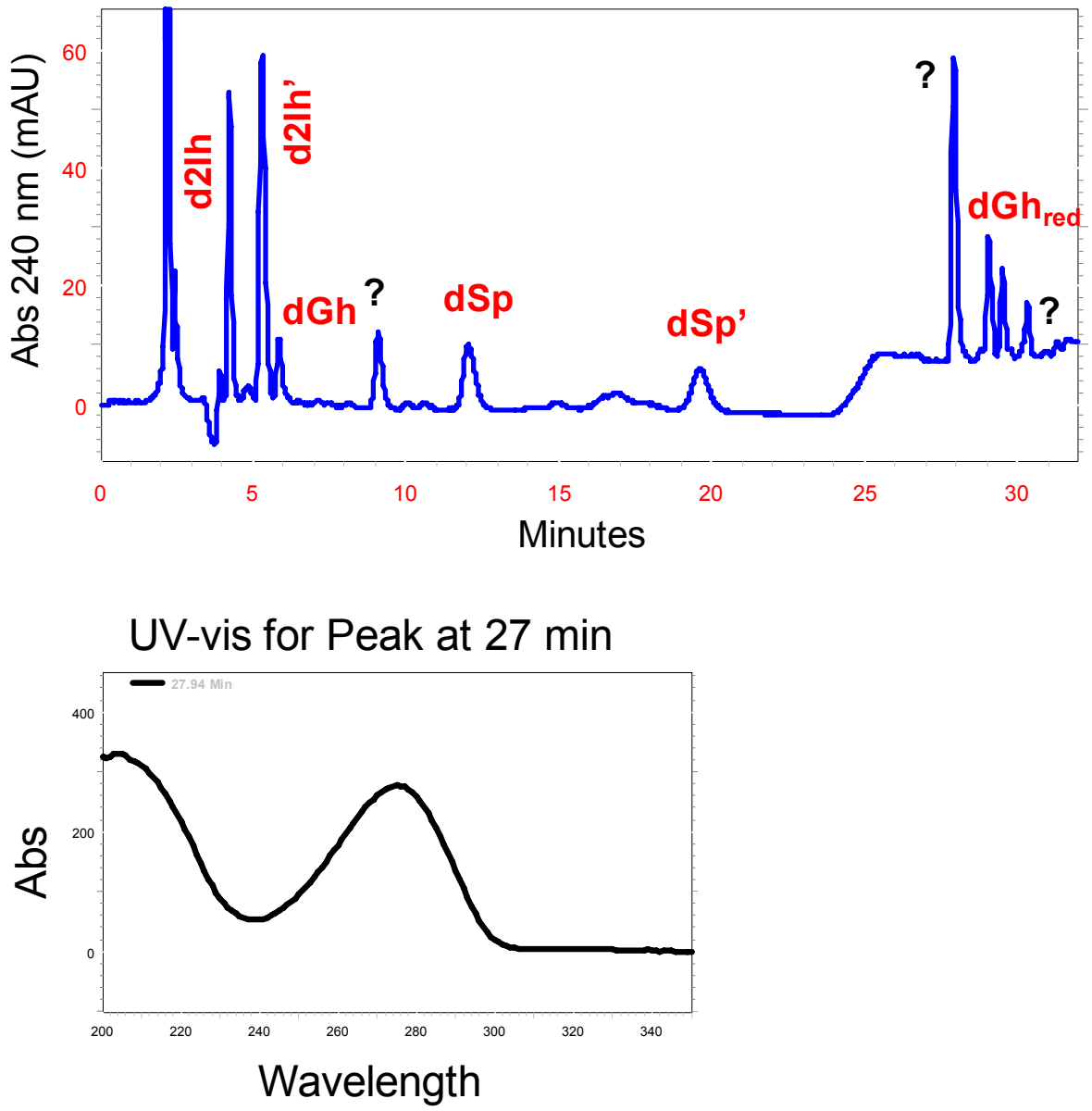

Figure S19. Hypercarb Column HPLC Chromatogram for the Digested **ODN-12** Oxidation Reaction. The peaks at 8 and 27 min were only observed in the **ODN-12** reactions. The peaks at 8 and 27 min would not ionize under the LC-MS conditions used; therefore, these peaks were not identified. Based on the UV-vis for the peak at 27 min this peak is still aromatic in nature, and could be the Cyt free base.

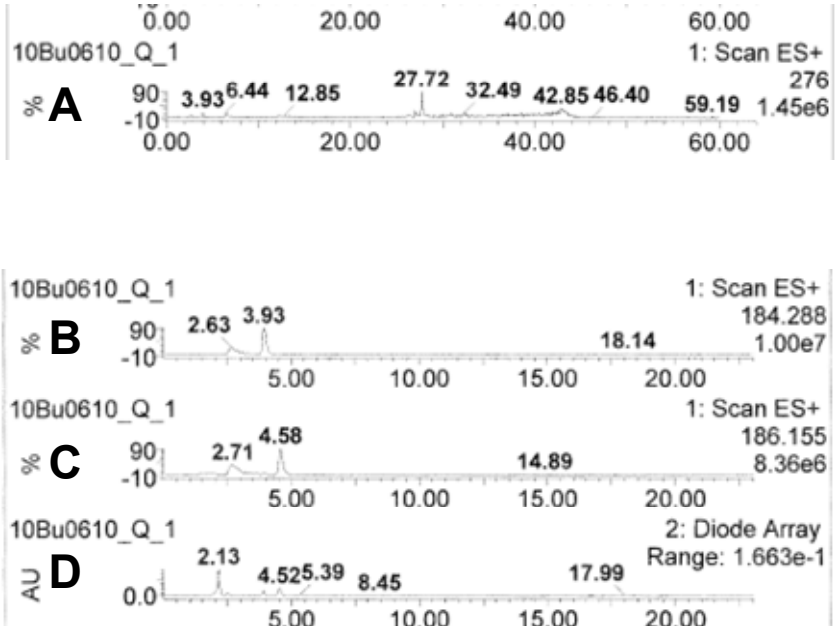

Figure S20. LC-ESI+-MS providing the additional masses observed from the double-stranded ODN reactions. Under the digestion conditions used to liberate the damaged nucleosides, the free bases Sp and 2Ih were also detected in low yields.

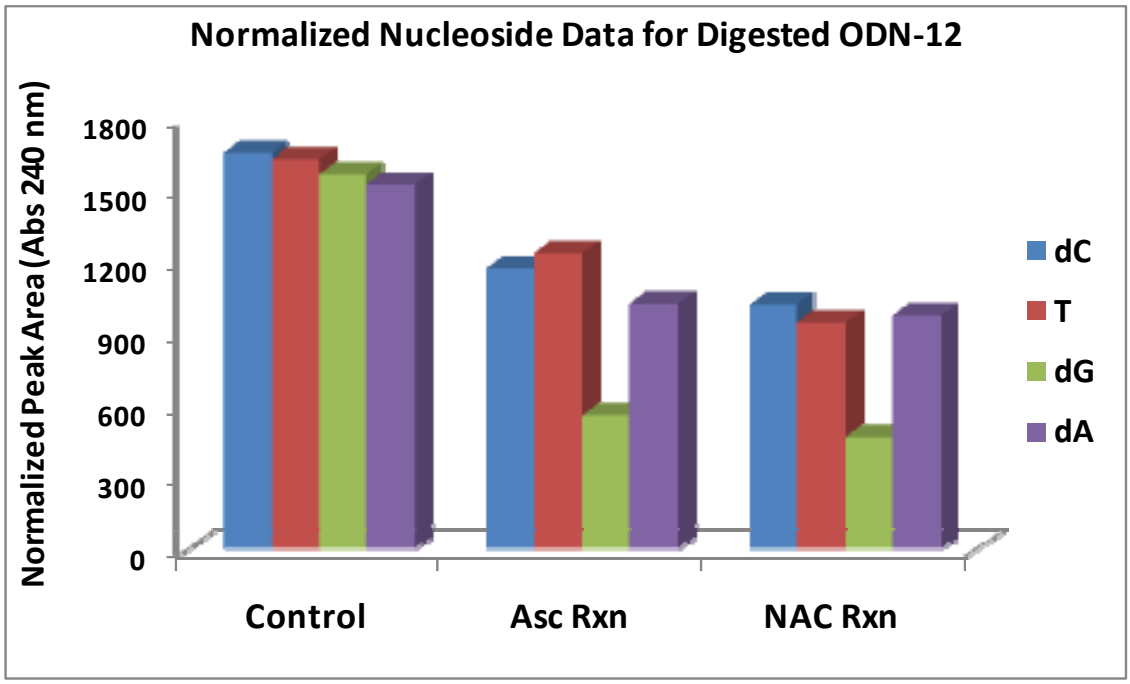

Figure S21. Average nuclease digestion yields for unreacted and reacted ODN-12 samples. Each value represents the average of three independent trials. The average error is 6-8% of the represented value.

		Cu(II)/H_2O_2/Asc		
Product	**dG**	**ODN-1**	**ODN-2**	**ODN-12**
Base Release	31.39564	19.395367	24.46995	8.5220018
dOG	14.8393	1.8842201	2.392463	0.9590188
dSp	12.99083	7.7131922	10.10812	7.7491579
dGh	2.062508	25.827973	29.45231	22.864582
dZ	3.009965	7.168343	7.884322	0
d2Ih	32.74689	38.010904	25.69284	50.574583
dGh_{red}	0	0	0	9.3306563
5',8-Cyclo-dG	2.954867	0	0	0
		Cu(II)/H_2O_2/NAC		
Product	**dG**	**ODN-1**	**ODN-2**	**ODN-12**
Base Rel	20.05199	10.448241	6.066097	14.986277
dOG	8.246686	2.1129247	0.53651	1.4775003
Sp	9.390157	13.021371	13.3403	8.6047029
Gh	2.526997	15.718857	15.90063	16.30966
Z	1.281349	11.604555	10.17867	0
2Ih	57.5164	47.094051	53.97779	51.390177
dGh_{red}	0	0	0	7.2316824
5',8-Cyclo-dG	0.986422	0	0	0

Figure S22. Relative product distributions from each reaction context studied. Each value represents the average of three independent trials that each have an error of ~5-6% of the reported value.

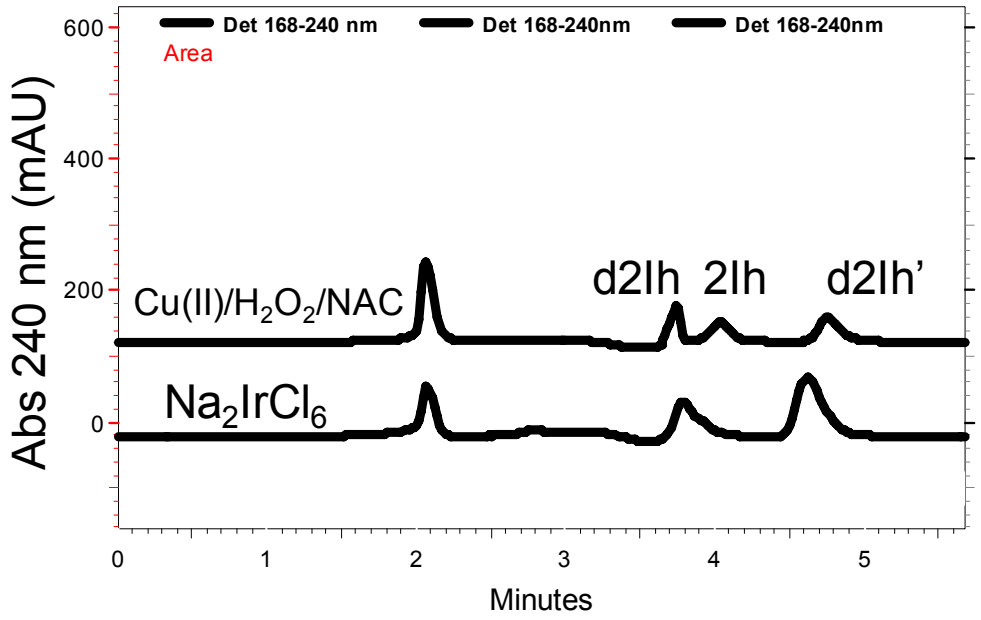

Figure S23. Oxidation of **d2Ih** with Cu(II)/H_2O_2/NAC (top HPLC trace) or Na_2IrCl_6 (bottom HPLC trace). The oxidation of **d2Ih** was conducted with the same conditions as used with **dG** (1.0 mM Cu(II), 2.0 mM NAC, and 10.0 mM H2O2), or **d2Ih** was attempted to be oxidized with 4 equiv of Na_2IrCl_6. Both reactions were conducted at 22 ^{o}C and pH 7.